ADVANCED FUNCTIONAL MATERIALS
www.afm-journal.de

Wear Mechanics of the Female Locust Digging Valves: The "Good Enough" Principle

*Andre Eccel Vellwock, Shai Sonnenreich, Shmuel Gershon, Yin Chang, Luca Bertinetti, Maryam Tadayon, Amir Ayali, Yael Politi, and Bat-El Pinchasik**

Adult female desert locusts (*Schistocerca gregaria*) dig underground to lay their eggs, ensuring optimal conditions for successful hatching. Digging is performed using the two pairs of oviposition valves at the tip of the female's abdomen. These valves are subjected to considerable shear forces during the repeated digging cycles, potentially leading to wear over time. The resilience of the valves is investigated by analyzing the relationship between digging experience and valve damage and wear throughout the female locust's life. The findings reveal the ability of the valves to withstand the significant shear forces encountered during digging. Despite this resilience, however, perceptible limitations in the valves' mechanical durability against wear are observed. Toward the end of the female locust's life, the valves show substantial signs of wear, indicating effective performance but with limited longevity, i.e., a designated life span that enables successful oviposition for *ca*. four oviposition cycles. A comparison of the valve material with that of the animals' mandibles, which are used continuously throughout their life and show remarkable wear-resistance, further highlights the evolutionary adaptation of the valve materials to their specific function, suggesting a trade-off between energetic investment and the sufficient, or "good-enough", performance that is required for survival.

1. Introduction

"Wear" in biology refers to the gradual degradation and breakdown of biological structures and materials due to mechanical forces, environmental conditions, and physiological processes, influencing the life span and functionality of organisms and their organs (or systems).[1–4] Wear in biological materials occurs in diverse forms and scales, from molecular interactions in microtubules[5] to macroscopic processes in organs such as teeth.[1,6] A wide variety of biological materials demonstrate enhanced wear resistance, particularly in systems subjected to high shear forces.[7,8] Insects that burrow into soil or wood, such as ants, termites, and certain beetles, have evolved wear-resistant body parts to withstand the abrasive effects of digging and tunneling.[9–11] Insects that are either predators, such as mantises and dragonflies, or grazers, such as ants and beetles, have evolved wear-resistant mouthparts or appendages to handle struggling prey and to protect against damage during feeding.

Several mechanisms in nature render biological materials wear-resistant. For example, spider claws exhibit high amounts of metal ions that cross-link an otherwise fully organic matrix, along with an exoskeleton composed of multilayered chitin-protein fibrils. Their claws, which facilitate hanging and locomotion on rough surfaces, can thus resist cyclic abrasion forces.[3] Similar adaptations are observed in spider fangs, responsible for piercing through other animals' tissues and thus necessitating withstanding local shear loads.[12] Distinct adaptations are also found in the mandibles throughout the arthropod phylum. In leaf-cutting ants, mandible wear can

A. E. Vellwock, Y. Chang, L. Bertinetti, M. Tadayon, Y. Politi
B CUBE—Center for Molecular Bioengineering
Technische Universität Dresden
01307 Dresden, Germany

S. Sonnenreich, S. Gershon, B.-E. Pinchasik
School of Mechanical Engineering
Tel-Aviv University
Tel-Aviv 6997801, Israel
E-mail: pinchasik@tauex.tau.ac.il

The ORCID identification number(s) for the author(s) of this article can be found under https://doi.org/10.1002/adfm.202413510

DOI: 10.1002/adfm.202413510

M. Tadayon
Department of Biomaterials
Max Planck Institute of Colloids and Interfaces
14476 Potsdam, Germany

A. Ayali
School of Zoology
Faculty of Life Sciences and Sagol School of Neuroscience
Tel-Aviv University
Tel-Aviv 6997801, Israel

B.-E. Pinchasik
Center for Physics and Chemistry of Living Systems
Tel-Aviv University
Tel-Aviv 6997801, Israel

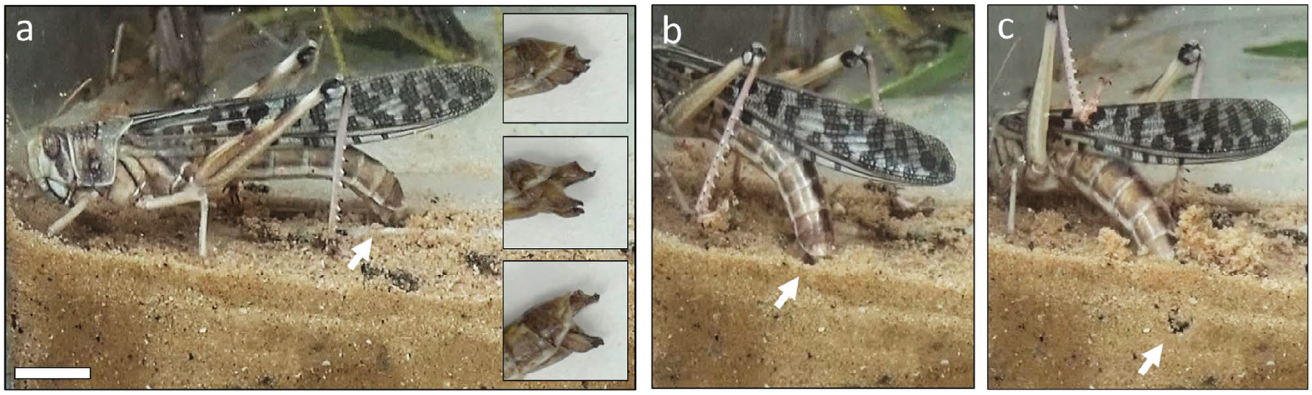

Figure 1. A female locust digging underground. a) The female finds a suitable spot to start digging. Inset: the cyclic opening and closing motion of the valves, used to create the underground hole. The white arrows indicate the position of the digging valves, located at the end of the abdominal region. b) The locust starts digging while extending the abdomen and c) propagates underground. The scale bar corresponds to 1 cm.

substantially affect the force required to cut leaves.[13,14] As in other arthropods, ant mandibles tend to be reinforced by metal ions (e.g., copper and zinc).[15,16] The locust mandible is reinforced with zinc and can self-sharpen due to its unique kinetics, whereby a scissor-like movement gradually sharpens the mandibles during feeding.[17]

The female locust employs a distinctive mechanism for digging and laying her eggs deep within the soil.[18] Utilizing two pairs of sclerotized valves, she displaces granular matter while extending her abdomen to navigate underground.[19–21] Upon reaching the desired depth (with respect to temperature and moisture), she deposits the egg pod (i.e., an agglomeration of eggs) followed by the secretion of the maternal foam. This process ensures the optimal conditions required for egg incubation, while also shielding them from potential predators. Oviposition may take place ≈3–4 times throughout the adult female's life. **Figure 1** depicts a female desert locust (*Schistocerca gregaria*) during oviposition. The female first locates a suitable spot, where she can start digging a hole (Figure 1a; the inset images show the cyclic motion of opening and closing of the digging valves). She then starts digging (Figure 1b) and propagating underground (Figure 1c) until finding a suitable place to lay the eggs. During the subterranean digging process, she can avoid obstacles by means of steering.[22] Previous studies have shown that the dorsal and ventral valves fulfill different functions during digging: the dorsal valves are responsible for the digging, and the ventral valves are used as an anchor while the abdomen extends, the ovipositor propagates, and the tunnel is created.[18–21].

There have been several efforts to characterize the biochemical composition, microstructure, and material organization of arthropod ovipositors. Metal ions have been detected in the ovipositors of some arthropods, such as cicadas,[23] but yet to be evaluated in the ovipositors of locusts. Blackwell and Weih studied the structural organization of chitin and matrix proteins in the ovipositor of the giant ichneumonid wasp using X-ray analysis.[24] Additionally, multiple studies have reported on the morphology and mechanical properties of ovipositors in other insects.[25–27] However, the relationship between material composition and functional performance of these structures remains unclear.

In this study, we examined the mechanisms and factors that drive wear in the digging valves of the female locust, exploring the relationship between nanoscale mechanical properties and micro- and macroscale wear of the structure. We found that the female's ovipositor valves are more compliant and less hard than her mandibles. The valves of young adult females broke and wore completely following exposure to three (artificial) wear cycles, while those of the sexually mature female locusts did not break but did demonstrate considerable wear after three digging cycles, possibly leading to much-reduced functionality. Nanowear tests revealed that the wear resistance of the valves is moderate, especially in comparison to the other cuticular appendages of arthropods. Our findings suggest that the female locust valves are "good enough" for their needs: i.e., while they have no extraordinary mechanical or tribological properties, they are able to perform digging throughout 3–4 oviposition cycles. These findings demonstrate that an animal's functional appendages in nature may be specifically "tailored" in terms of structure and materials –, i.e., appropriately designed to fulfill their purpose – possibly minimizing energy expenditure and the use of valuable construction materials. Our findings offer valuable material and mechanical considerations for the development of innovative non-drilling burrowing tools. Such designs in nature can inspire 3D-printed anisotropic materials, leveraging composites and tailoring properties to improve the properties of synthetic materials beyond those of the digging apparatus.[28,29]

2. Results and Discussion

2.1. Wear of the Female Locust Valves Depends on Age and Digging History

The morphology of the dorsal and ventral digging valves of the female locust undergoes changes at different stages of adult life (**Figure 2**). In this study, we evaluated the valves of females at 7 days and 30–40 days post adult emergences. Valves with no oviposition history (namely, no digging attempts), present a sharp edge and a pointed tip (Figure 2a,b). However, after only four oviposition digging cycles in granular matter (natural construction sand with ≈15% water content), the tips and edges of the valves become rounded due to wear (Figure 2c).

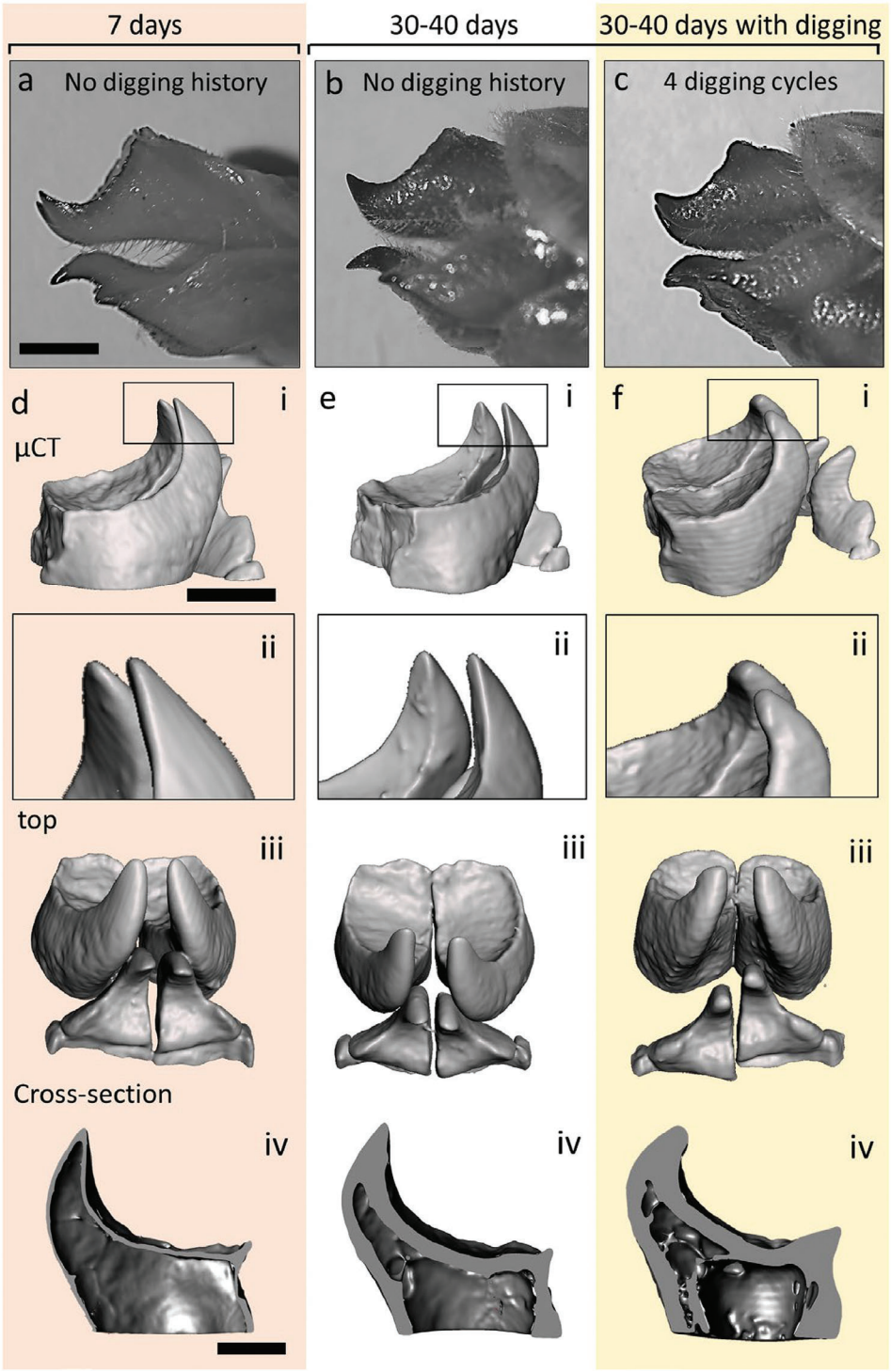

Figure 2. Wear of the female locust digging valves. a–c) Optical micrographs and d–f) computed tomography micrographs of valves from (a,d) a young adult female locust without oviposition history; sexually mature females (b,e) without oviposition history; and (c,f) after four digging cycles. Scale bars in (a–c) and (d–f) correspond to 2 and 1.75 mm, respectively.

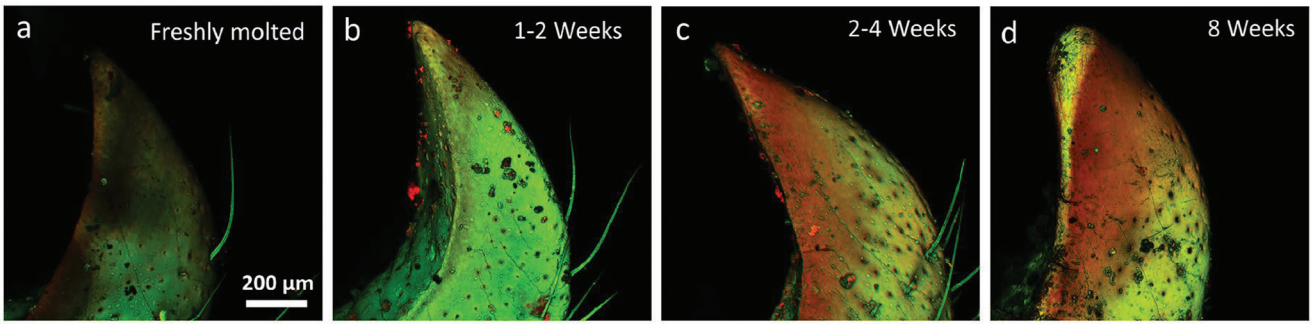

Figure 3. High-resolution confocal micrographs of the female locust valves. a) Freshly molted adult female, b) 1–2 weeks post adult emergence, c) 2–4 weeks post adult emergence, d) 8 weeks post adult emergence, following 3–4 digging cycles. The green areas indicate cuticular materials such as chitin, and the red areas correspond to sclerotized regions, known for their enhanced mechanical properties.

Computed tomography (CT) reconstruction provides a 3D view of the valves' tips at a higher resolution (Figure 2d–f). Here, the disparity in geometry between structures lacking a history of digging (Figure 2d,e) and those with such a history (Figure 2f) is evident, particularly in the roundness of the edges after four digging cycles.

Sclerotization is the process in which the cuticle becomes hardened and stiffer through (bio)chemical cross-linking of proteins. This process is also accompanied by drastic dehydration,[30,31] and is often associated with changes in autofluorescence of the cuticle.[32,33] We used high-resolution scanning laser confocal microscopy to qualitatively map the material composition of the valves at different stages of the female locust's life. **Figure 3** depicts the tip of the dorsal valve from a freshly molted adult female up to 8 weeks post molting. Such females usually have a history of 3–4 oviposition cycles.

From the adult eclosion and up to 1–2 weeks afterward, the valves are very mildly sclerotized (Figure 3a,b), indicated by the dominant autofluorescence in the green region (516 nm).[31] After a few weeks, the dorsal (distal) area of the valve becomes sclerotized, as indicated by the increase in red autofluorescence (654 nm) (Figure 3c), suggesting enhanced stiffness and mechanical stability.[19,31] After several digging cycles, significant wear of the valve is visible (Figure 3d). In addition to the rounded shape of the tip, also indicated by the CT scans (Figure 2f), the highly cross-linked sclerotized area is worn, sensory hairs are broken, and the internal material is exposed (appears green in Figure 3d).

2.2. The Biomechanics of the Female Locust Valves

2.2.1. Macromechanical Properties

The wear resistance of the valves was examined using an ad-hoc friction test (**Figure 4**). The valves of female locusts at 7 days and 30–40 days post-adult emergence were tested by dragging them against an abrasive paper at a constant velocity (Figure 4a,b). Three valves at a time were fixed onto a disk, positioned on one plane. Their mechanical response was averaged (Figure 4c; Figure S1, Supporting Information). The valves were oriented so that their tips received the initial abrasion during the test (Figure 4d). Although the contact conditions of the valves on the sandpaper differ significantly from the digging of the female locust in granular matter, the test allowed us to directly measure the friction forces while concomitantly applying a preload (force normal to the valves) that is comparable to the forces acting on the valves of the female during digging.[19] For the calculations of the static and kinetic friction coefficients see Supporting Information and Figure S1 (Supporting Information).

The friction force was measured using a load cell. The friction coefficients were then calculated from the known setup weight. The static and kinetic friction coefficients corresponded to the states before and during the motion of the valves against the surface, respectively. After each test, the valves were optically imaged to visualize the wear on the tip (Figure 4f,g). As expected, the static coefficients were higher than the kinetic ones. Furthermore, the valves of the 30–40-days-old females showed relatively lower wear compared to those of the younger ones. Under the same experimental condition, the valves of the 7-day-old females appeared to have experienced tear and distortion in addition to wear, suggesting that the valve surfaces that contact with the ground may have deteriorated almost completely by the third digging cycle (Figure 4g).

2.2.2. Nanomechanical Properties

Nanoindentation techniques were utilized to investigate the nanomechanical properties of the valves. The female locust mandibles, known for their increased wear resistance, were tested for comparison. Unlike the digging valves, mandibles must maintain daily functionality to support feeding throughout the animal's lifetime.[34–37] Nanowear tests were conducted on both the longitudinal and transversal sections of the dry valves and mandibles. Evaluation of the worn depth, indicative of local abrasion effects, revealed higher levels of wear in the valves compared to the mandibles (**Figure 5**).

The female locust's ovipositor valves are less wear-resistant than her mandibles. When compared, for example, to the spider's appendages (e.g., claws and fangs), known for their high wear resistance,[3] the locust valves show one to two orders of magnitude higher worn depth (20–30 nm compared with

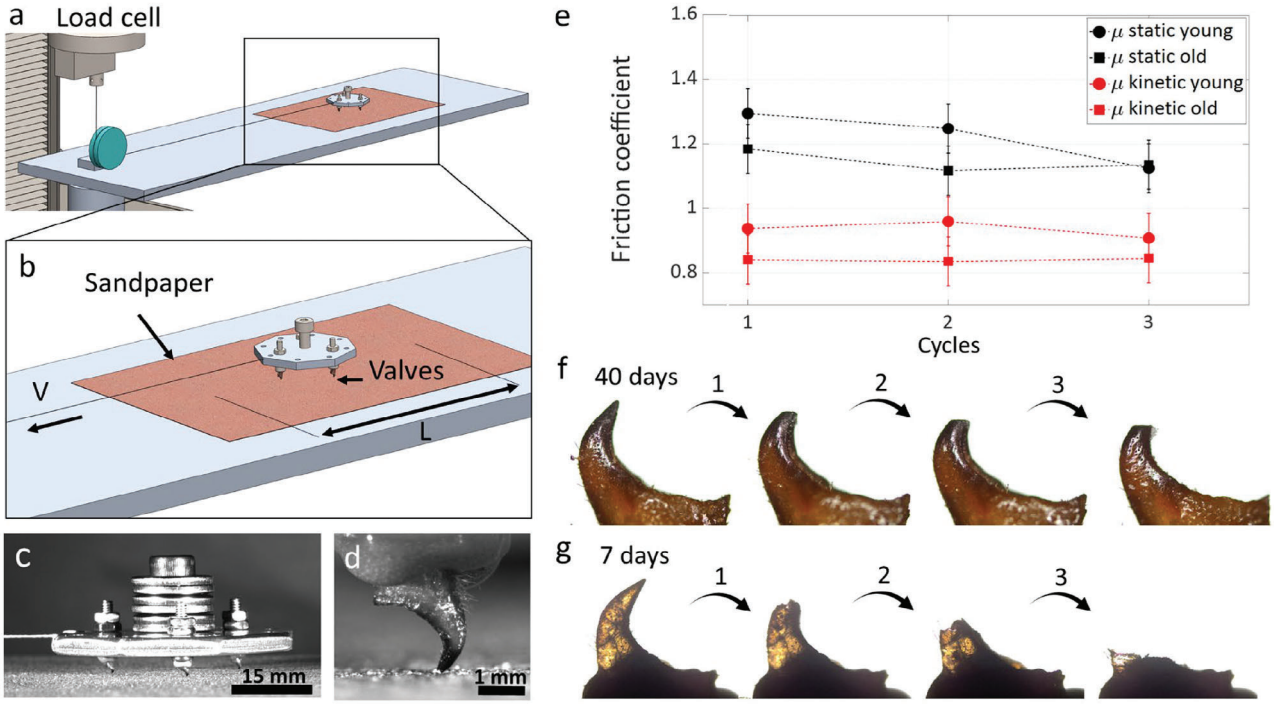

Figure 4. Macroscale friction test of 7-day-old and 30–40-days-old locust valves. a,b) The experimental setup comprised a load cell connected to a sample holder containing three valves from females of the same age, through a mechanical pulley. c) A side view of the sample holder, with the mounted valves, and d) a higher magnification of the contact between the valve and the rough surface. e) Static and kinetic friction coefficients of the valves. Optical images of the f) old and g) young valves after each cycle.

200-1700 nm worn depth, respectively). Nanowear tests revealed that the valves have lower wear resistance at their base (regions L3), independently of age, with worn depth reaching 1705 ± 178 nm. Moreover, the highest wear-resistant results for both ages were obtained in the transversal section, demonstrating that wear-resistant properties are anisotropic. Interestingly, in the mandibles, the longitudinal sections outperformed the transversal ones, with a worn depth as low as 34 ± 5 nm, comparable with that in spider fangs and claws. In contrast to the results from macroscale friction tests, surface abrasion showed no significant variation between the 7-day-old and 30–40-days-old valves. We note that the mechanical load (e.g., loading regime, contact geometry, abraded area) and the type of failure (wear vs wear + brittle failure) associated with these two experiments differ considerably.

Nanoindentation grids (under dry conditions) were utilized to assess the material properties of the valves, including reduced modulus, hardness, and wear-resistance index. This evaluation

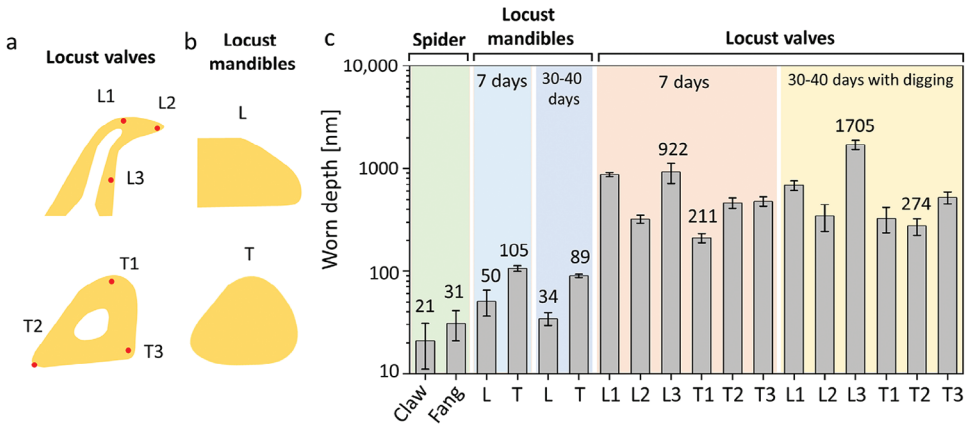

Figure 5. Nanowear of the female locust valves and mandibles, compared to other arthropods. Worn depth (inversely proportional to wear resistance) following nanowear tests on different areas of the longitudinal and transversal sections of the dorsal valves and mandibles, in comparison to literature reports on spider claws and fangs.[3]

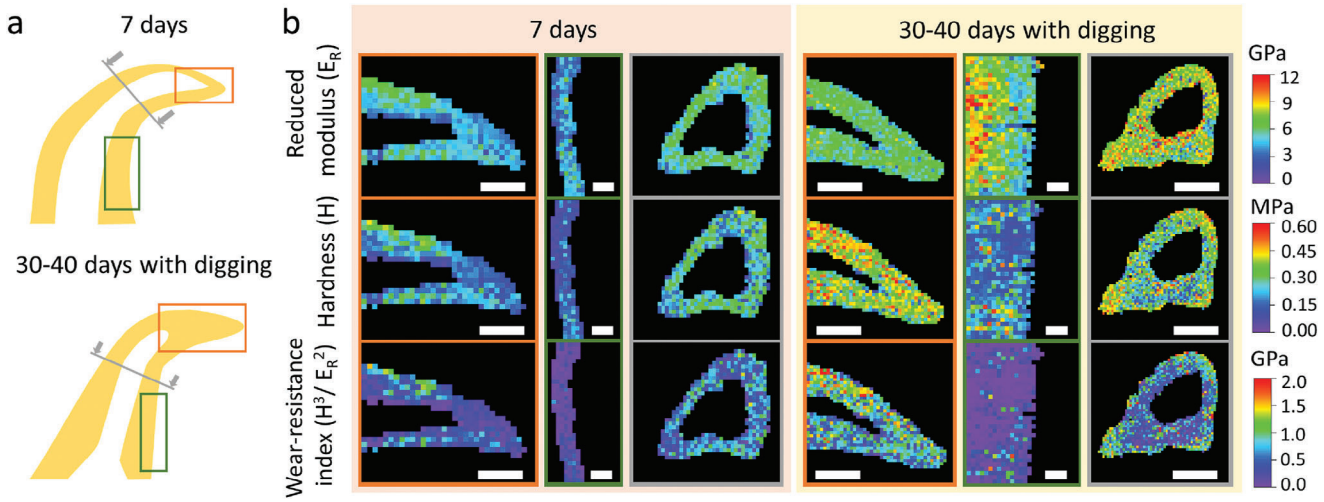

Figure 6. Nanoindentation characterization of the female locust valves. i) A 7-day-old valve has a more compliant and softer material than a-ii) 30–40-day-old valve with digging history. The wear-resistance index indicates that the older structure was better able to withstand abrasion, especially at longitudinal sections and edges of the transversal sections. Scale bars: 50 µm.

was conducted across specific regions of interest: the tip and base in longitudinal sections, marked in **Figure 6**a by orange and green frames, respectively, and the transverse section (grey line).

Already at 7-days post adult emergence, the valve tip exhibited higher stiffness and hardness compared to its base. Local variations were observed in the tip, featuring reinforcements in both the concave and convex regions. Higher modulus and hardness values were measured in the transversal than in the longitudinal sections, again revealing the high material anisotropy. Wear resistance prediction, through evaluating the H^3/E_R^2 ratio,[1] suggested that the base is the least wear-resistant region, in agreement with the nanowear tests (Figure 5). At 30–40-days old, the material was much stiffer and harder than at 7-days, possibly related to increased sclerotization, as suggested by the autofluorescence imaging. Aging introduced a two-fold increase in modulus. In addition, a 2-3-fold increase in hardness was observed at the tip and at the transversal section, especially at its edges. The wear resistance index (H^3/E_R^2) suggested possible regions with increased wear resistance. These findings are in agreement with the experimental nanowear analyses (Figure 5).

The mechanical properties of the cuticle are influenced by tissue humidity, resulting in a softer and more compliant behavior following hydration.[38,39] The precise local moist content of the cuticle, however, remains unknown. While the desert locust primarily inhabits dry desert climates, its valve lumen (i.e., the inner hollow area) remains in constant contact with the hemolymph. Drying can lead to complex changes in cuticle mechanical behavior, as some regions may be more affected than others. Thus, to complement our findings from dry conditions, nanoindentation grids were conducted on 30–40-days-old valves in water (see experimental section). The results revealed a significant decrease in modulus and hardness compared to those from the dry assessment. Nonetheless, specific regions, such as the edge region in the transversal section, still exhibited an increased H^3/E_R^2 ratio (bottom left in Figure S2, Supporting Information).

2.2.3. Microstructural Characterization

The internal architecture of the valves was visualized using cryofracture scanning electron microscopy (**Figure 7**; Figure S3, Supporting Information). Locust valves from a female at 7-days post adult emergence reveal a thin exoskeleton (Figure 7b) relative to that of their 30–40-days-old counterparts (Figure 7f). This finding was corroborated by weight measurements of the whole valves upon maturation (Figure S4, Supporting Information).

In the transversal section, a characteristic helicoidal fiber architecture was observed in the innermost layer of the young valve (Figure 7c). The middle and thicker layer is attributed to the exocuticle, with anisotropic texture (due to chitin-fibrils, see below) oriented almost radially and perpendicular to the valve surface (Figure 7d). Although the outmost layer, the epicuticle, does not contain chitin, it also presents textural anisotropy (Figure 7e). The extended thickness of the endocuticle (the innermost layer) in 30–40-day-old valves (Figure 7f), relative to the 7-day-old valves, in contrast, is related to the cuticle deposition that begins following ecdysis and continues for several weeks. As already seen in the 7-day-old valves, the endocuticle displays a typical helicoidal architecture (Figure 7g,h), with the lamella oriented parallel to the valve surface (Figure S5, Supporting Information). In the young valves, the exocuticle also presents radial orientation, but here the layer is less thick (Figure 7h). This difference is not related to the age differences between the samples, but to the fracture position along the valve (as the exocuticle is not remodeled following ecdysis). This anisotropy in the epicuticle is also evident in the fractured 30–40-days-old valve (Figure 7i) and attributed to the alignment of proteins, rather than chitin. Scanning microfocus X-ray diffraction analysis similarly revealed chitin fiber orientation almost orthogonal to the valve surface in the exocuticle (Figure 7j; Figure S6, Supporting Information). Interestingly, this type of fiber orientation is also seen in the mandibles of crayfish, but not in those of the studied locust species.[40] The longitudinal section (Figure 7j) shows that the thickness of this layer increases from the tip toward the base, in

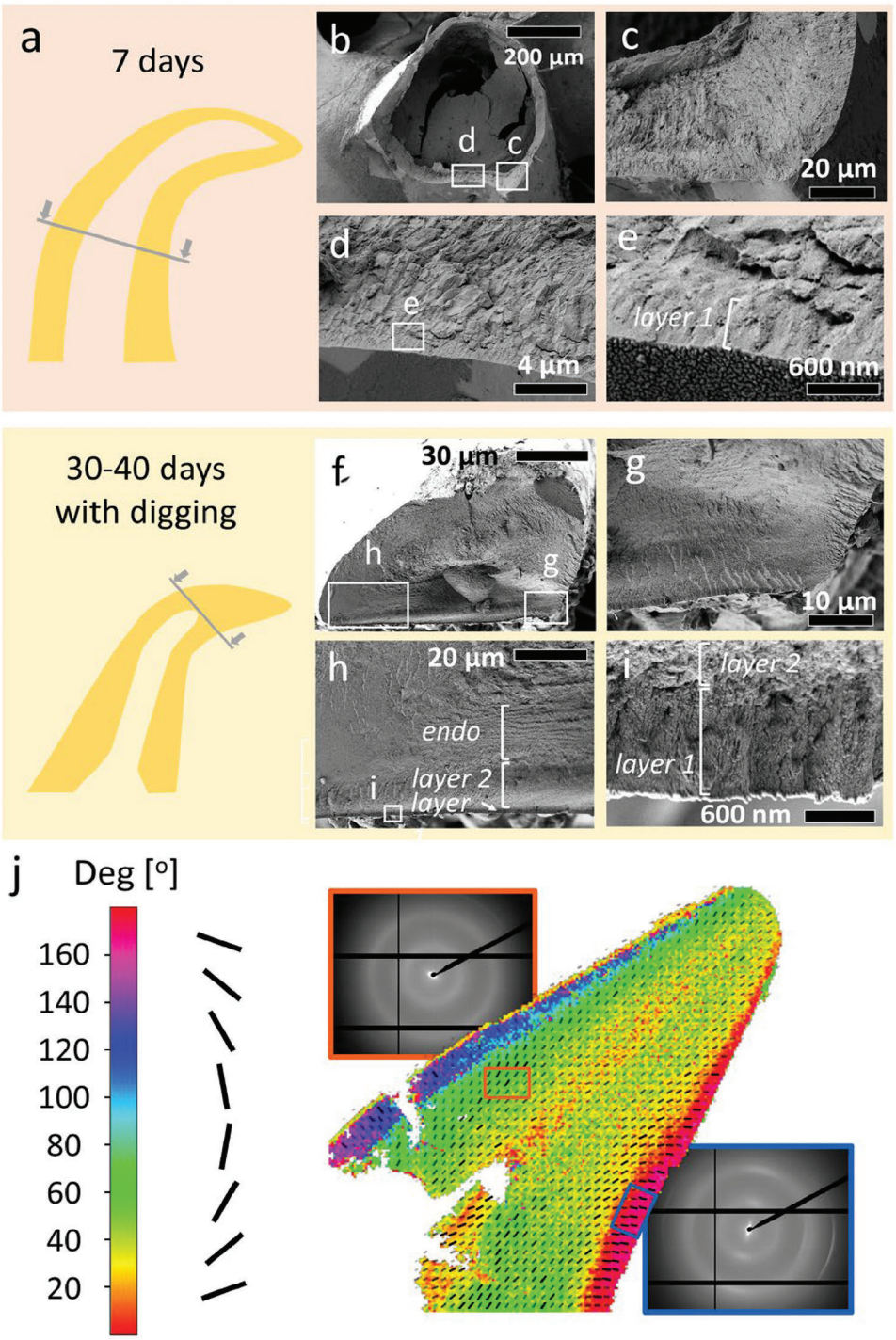

Figure 7. Tissue architecture of the valves. a–i) Scanning electron micrographs of cryofractured valves reveal contrasting cuticle thickness and a layered formation. (a–e) In the 7-day-old valve, the structure is predominantly composed of a helicoidal fiber architecture. The outermost layer (layer 1) displays a distinct topography attributed to the epicuticle. (f–i) In the 30–40-days-old valve, the endocuticle is clearly visible, along with two contrasting layers (layer 1 and layer 2) that highlight differences in topography. Layer 2 is likely the exocuticle, while layer 1 is the epicuticle. The chitin-absent epicuticle shows topography alignment, attributed to the orientation of proteins. j) Fiber orientation mapping and representative, averaged 2D XRD diffraction patterns of a longitudinal section of 30–40-days-old valves with a digging history. The color-coded vector plot indicates that the outer (red) layer has a contrasting chitin-fibril orientation compared to the inner (green) layer. Additionally, the XRD patterns demonstrate a stronger orientation in the outer region, as indicated by the more intense reflections, while the inner region shows a weak alignment.

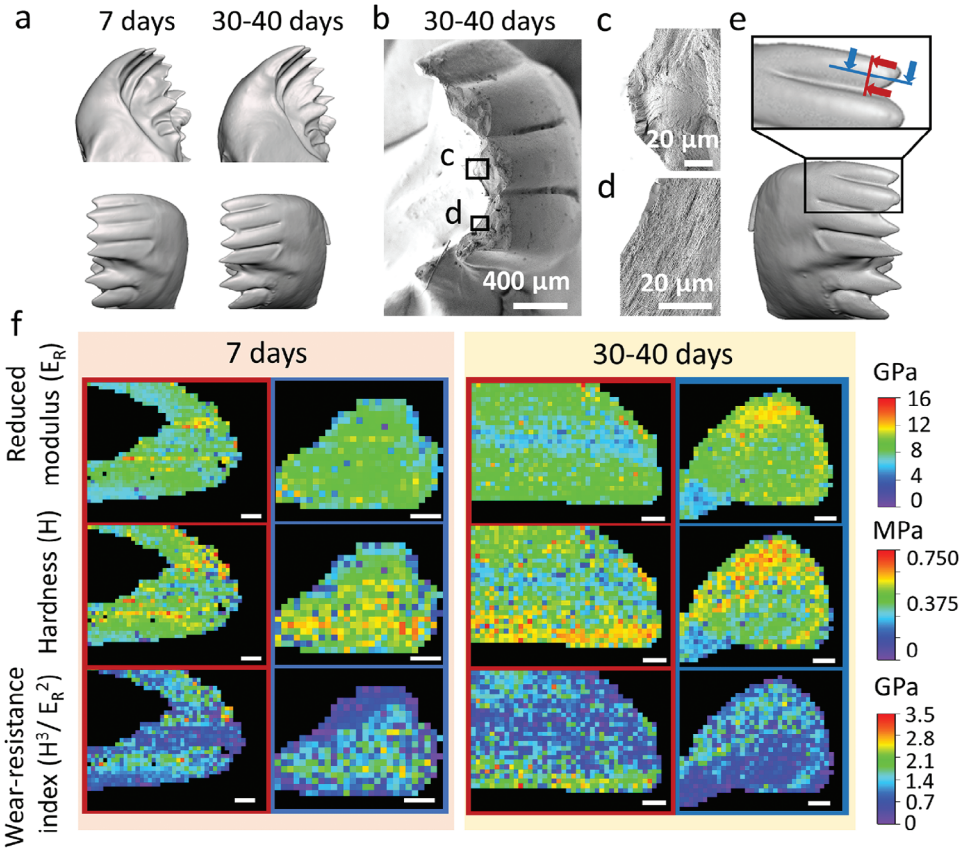

Figure 8. Characterization of mandibles of female locusts. a) Computed tomography micrographs of mandibles at 7 days and 30–40 days old. b) Cryo-fracture imaging of the adult mandible, demonstrating a c) intricate and d) compacted chitin-based lamellae architecture. At both ages, the mandible first tooth was e) sectioned and probed to assess its f) nanomechanical properties.

agreement with SEM observations. Furthermore, the anisotropy can be seen in the exocuticle in both the longitudinal (Figure 7j) and transverse sections (Figure S6, Supporting Information), indicating that the fibers are not directly perpendicular to the surface but oblique to it (out of plane relative to the valve section in both orientations). The endocuticle, in comparison, presents a relatively weak anisotropic signal against a background of a mostly isotropic signal, consistent with a rotated plywood architecture as observed in SEM.

2.2.4. Elemental Composition

Energy-dispersive X-ray spectroscopy (EDS) was performed to further evaluate the elemental composition of the valves (Figures S7 and S8, Supporting Information). Other than the typical elements found in the biological samples, such as carbon, oxygen, and nitrogen, we found no metal ions above the detection limit of the instrument (≈1–2% wt.), but a limited presence of chlorine.

2.3. Evaluation of the Female Locust Valve in Comparison to the Mandible

Material wear constitutes a constant problem for organisms in general, and specifically for insects. Desert locusts feed on various grasses whose leaves often contain silica or other abrasive materials. Interestingly, abrasion caused by the opposite mandibles during mastication was suggested to lead to self-sharpening, which can help maintain mandible functionality over time.[17] Thus, the locust mandibles experience daily recurring shear stresses but show local adaptations to sustain or resist associated damage. We therefore compared the wear resistance of mandibles to that of the ovipositor valves from 7-day-old and 30–40-days-old female desert locusts. Micro-CT imaging revealed minimal worn regions for both ages (**Figure** 8a), differing greatly from the results obtained for the valves (Figure 2). While investigation of the internal architecture revealed the chitin-protein fibrils structure, with a compacted lamellae region (Figure 8b), as observed in the valve endocuticle (Figure 7), a specialized exocuticle with orthogonal fiber orientation was not observed. To further analyze the material, longitudinal and transversal sections of the mandible first tooth were prepared (Figure 8e). At 7 days old, nanoindentation grids revealed a quasi-homogeneous stiffness of 8.12 ± 1.56 GPa. On average, the tissue presented a hardness of 0.40 ± 0.11 GPa, with local variations, translating to a wear-resistance index of up to 1.09 ± 0.57 MPa. At 30–40 days old, the longitudinal section displayed stiffer (8.60 ± 1.54 GPa) and harder (0.42 ± 0.11 GPa) regions, especially on the concave side.

In the transversal section, the tooth had a higher modulus and hardness on the convex side of the mandible. This change in

the location of the reinforced region most likely resulted from the position of the sectioning. Nevertheless, both of these areas confirm previous reports demonstrating the presence of wear-resistant material in the mandibles. Elemental analysis of 7-day-old mandibles revealed the presence of chlorine but, surprisingly, an absence of zinc (Figures S8 and S9, Supporting Information). While the chlorine spatial distribution matched the regions of higher hardness, the chemical state of chlorine in the sample remains to be determined. It is possible that chlorine incorporation is related to sclerotization,[41] indicating an indirect relationship between chlorine distribution and increased hardness. In 30–40-days-old valves, the presence of zinc is correlated with that of chlorine (Figures S8 and S9, Supporting Information), as well as increased hardness and modulus. In comparison to the digging valves, the mandibles exhibited greater stiffness, hardness, and wear resistance, regardless of tissue age. This is mainly attributed to sclerotization and the inclusion of zinc, both of which serve in local mechanical reinforcements.

3. Conclusion

The stiffening and hardening process of the female locust's digging valves is essential to enable the insect to effectively burrow underground and deposit her eggs. This transformation is tuned to withstand the wear and tear that occurs during multiple digging cycles throughout the female's lifetime. The valves, however, are neither exceptionally stiff nor hard, and after merely 3–4 digging cycles the sharpness of their tips diminishes to a worn-out state. In comparison to the locust's mandibles and the spider's appendages, such as claws and fangs, the wear resistance of locust valves is notably lower by 1–2 orders of magnitude. While macroscopic friction tests underscored complete breakage after 3 digging cycles in valves of young females, they also revealed a maturation of materials, such as endocuticle growth and sclerotization, which provide resistance to damage in mature females. Unlike other wear-resistant structures found in arthropods, elemental analysis revealed a lack of the relevant metal-ion cross-linking that is typically associated with increased local mechanical properties such as hardness, stiffness, and wear resistance. The absence of metal ions may reflect a trade-off in the locust's biology. Incorporating metal ions into the cuticle could require additional energy and nutrient resources, which might be more effectively allocated to other physiological functions, particularly given the limited use and lifespan of the digging valves. Cryo-fracture and XRD results, however, revealed an uncommon material architecture, with chitin fibers oriented perpendicular to the surface of the valve. In essence, the valves are clearly not equipped to endure a continuous abrasion load over a long period of time. This is in accord with the egg-laying frequency of female locusts, which takes place only 3–4 times during the adult lifespan. This can be well understood in the context of the "good enough" principle, in which the structures are tailored to meet the functional requirements of the organ, without being "over-designed." Indeed, the biological structure of the locust ovipositor valves is not required to endure more than a few oviposition cycles. Given that the same species is genetically equipped with the biochemical and cellular machinery to produce more wear-resistant materials, as demonstrated in the composition of their mandibles, we anticipate that the "good-enough" architecture probably requires less energy or metabolic expenditure to develop. As has been previously suggested,[42] this offers an interesting lesson for designing man-made structural and sustainable components. This shift in perspective to "good enough" holds relevance for structural engineering, architecture, and product design, emphasizing the importance of efficiency and minimalism in material usage for a more sustainable world. Whether this alignment between function and materials arises from an evolutionary adaptation to the materials or, vice versa, the evolution of materials is aimed at accommodating function, remains an intriguing and open question.

4. Experimental Section

Experimental Insects: Locusts were obtained from the desert locust, *Schistocerca gregaria*, colony at the School of Zoology, Tel Aviv University. Females were of two different age groups: I) Young, premature females (age = 3–7 days post-ecdysis to adult); and II) Sexually mature females (age = 30–40 days post-ecdysis to adult). Females of the older-mature group were either kept in the regular breeding cages or housed under similar conditions but in dedicated smaller cages that allowed monitoring their oviposition history. Accordingly, the latter were further divided into two groups: 1) Females with no oviposition history (no access to oviposition substrate); and 2) Females with monitored oviposition history (e.g., four rounds of successful digging and oviposition).

Images and video sequences of the female locusts' oviposition behavior were obtained by tracking several gravid females in a glass-walled cage and capturing oviposition attempts near the wall. The details of the valves' motion were captured separately from several females by severing the ventral connectives anterior to the abdomen and thus releasing the motor pattern from descending inhibition.

Oviposition Valves and Mandibles Preparations: To obtain the oviposition valve samples, females were first anesthetized under CO_2. Following rapid dissection, the oviposition valves were air-dried for 48 h and then maintained in sealed Eppendorf tubes until use (imaging, testing, etc.). Samples of female locust mandibles were dissected and prepared following a similar procedure. Further sample treatment, imaging, and testing method-specific preparations are detailed below.

μCT Scan: All scans were performed using an X-ray computed tomography system (XT H 225 ST, Nikon Metrology NV, Leuven, Belgium), operated using a 225 kV 225 W reflection target, utilizing the following scan parameters: isotropic voxel size of 5 μm, 180 kV, 27 μA, no filter, 3141 projections, 500 ms exposure time, at the Shmunis Family Anthropology Institute, Dan David Center for Human Evolution and Biohistory Research, Sackler Faculty of Medicine, Tel Aviv University. A total of 18 samples were scanned.

Friction Measurements: To perform macroscale friction measurements, a 68sc-05 universal testing machine (Instron, Norwood, USA), coupled with a 2530—5 N load cell (Instron, Norwood, USA) and an additional part for friction measurements, were used for the wear tests. A p280 abrasive paper (Norton, Worcester, USA) was glued onto an acrylic surface. A Super Pe 15 lb fishing line (Sunline, Iwakuni, Japan) was used for load transfer. Three valves were affixed each time to the sample holder using Poxipol glue. After each test, the valves were imaged using a BX53M optical microscope (Olympus, Tokyo, Japan).

High-Resolution Laser Scanning Confocal Microscopy: Laser scanning confocal microscopy was performed with an LSM 880 (Zeiss, Jena, Germany) equipped with an Airyscan fast detector, together with 10× objective lenses (Zeiss, Jena, Germany) with argon and neon-helium lasers (wavelengths 488 and 633 nm, 90 % intensity). The intensities of the lasers and the detector gain were kept constant between samples.

Nanoindentation: Samples were embedded in epoxy resin and subjected to stepwise mechanical polishing, then probed with a nanomechanical tester (Triboindenter TI-950, Hysitron, USA) using a conospherical diamond tip with a radius of 1 μm. The tip indents were loaded at a

rate of 50 μN s^{-1} for 2 s until 100 μN, and held for 1 s, followed by unloading at 50 μN s^{-1} for 2 s. A grid of indents was performed for each sample, with a spacing of 10 and 20 μm, in either dry or hydrated conditions. The latter was performed with the sample fully submerged in deionized water. The results were analyzed according to the Oliver-Pharr model to extract the reduced modulus and hardness of the samples. Property maps were plotted using Origin 2019b (OriginLab, Northampton, USA).

Nanowear: The samples used for nanoindentation under dry conditions were also subjected to nanowear tests, in which the 1 μm tip, under a constant load of 350 μN, abraded a 5 μm × 5 μm area 30 times at a 2 Hz sliding rate. To calculate the worn depth, scanning probe microscopy (SPM) was performed to determine the surface of the abraded area. FIJI software was applied to calculate the worn depth, by comparing abraded and non-abraded heights.

EDS: For energy dispersive X-ray spectrometry (EDS), samples were coated with a 10 nm carbon layer using a MED 020 coater (Leica microsystems, Wetzlar, Germany). Data were acquired using a Crossbeam 550 (Zeiss, Jena, Germany) equipped with a Ultim Extreme detector (Oxford instruments, Oxfordshire, UK) with an acceleration voltage of 15 keV and a probe current of 100 pA. Acquisition was performed for 30 min. Results were analyzed and color-coded using AZtech software (Oxford instruments, Oxfordshire, UK). The counts graph was plotted considering only the area where the sample was located.

Cryofracture: Cryo SEM was performed on a Crossbeam 550 (Zeiss, Jena, Germany) equipped with a PP3010 cryo preparation system (Quorum Technologies, East Sussex, UK). The base of each valve was fixed to a holder using modeling clay and an equal part mixture of optimal cutting temperature (OCT) embedding compound (Cryostat Embedding Medium, Scigen, USA) and Colloidal Graphite (CG), (Aquadag Colloidal Graphite ECO, Agar Scientific, UK). Following fast cooling of the sample in slush nitrogen, the mixture solidified, stabilizing the sample. Samples were fractured in the cryo preparation chamber where the rigid rotating blade was manually displaced, impacting the valve. Although the region of impact between the blade and valve could be roughly controlled, the fracture did not necessarily always occur at the exact point of contact. To ensure electrical conductivity and reduce charging artifacts during imaging, the sample was platinum coated in the cryo preparation chamber, for 60 s at 5 mA, before imaging. For SEM imaging, an accelerating voltage of 1.5 kV and a probe current of 400 pA was set. The sample holder was kept at −140 °C and the anticontamination device at −175 °C.

XRD: Dried adult ovipositor samples were embedded in resin blocks and microtomed in a UC6 ultramicrome (Leica, Wetzlar, Germany) in cross-sectional and longitudinal directions, with each section 50 mm thick. Sections were attached to a silicon nitride (Si_3N_4) membrane and measured at the nanobranch of a dedicated SAXS/WAXS/XRF station of the ID13 beam line at the synchrotron ESRF (European Synchrotron Radiation Facility, Grenoble, France). An X-ray energy of $E_x = 13$ keV was chosen from the synchrotron radiation spectrum by a multilayered monochromator. XRD was performed with a beam cross-section of 70 nm × 70 nm and a 2 μm scanning step size in both *x* and *y* direction with 50 ms exposure time per point. Quartz powder was used to calibrate the sample to the detector distance. ESRF experiment number: SC-5329. The dataset can be accessed online.[43] Fiber orientation maps were obtained as follows: first, at each pixel of the map, the coordinates of the points in the detector image that displayed an intensity higher than the 99.5 percentile were extracted. The eigenvectors of this set of points were then calculated using the Principal Component Analysis (PCA) from the Scikit-learn library.[44] The angle at each point of the map was calculated by adding 90° to the orientation of the eigen vector with the largest eigen value.

Supporting Information

Supporting Information is available from the Wiley Online Library or from the author.

Acknowledgements

A.E.V. and S.S. contributed equally to this work. The authors are grateful to Keren Levy for assisting in maintaining and monitoring the female locusts; to Carolin Fischer for assistance during cryofracture; and to Dr. Aurimas Narkevicius, Carolin Fischer, and Dr. Oliver Späker for their support during the experiments at the synchrotron. The authors also thank Bar Ergaz from Ayelet Lesman Lab for assistance with confocal imaging. The authors acknowledge the European Synchrotron Radiation Facility (ESRF) for the provision of synchrotron radiation facilities under proposal number SC-5329, and the authors thank Alexey Melnikov for assistance and support in using beamline ID13. This research was supported by grants from the German Research Foundation (Deutsche Forschungsgemeinschaft DFG, PO 1725/10-1 and TA 1717/2-1) and the Maria Reiche postdoctoral fellowship of TU Dresden financed by the Free State of Saxony and the Federal and State Program for Women Professors (Professorinnenprogramm).

Conflict of Interest

The authors declare no conflict of interest.

Data Availability Statement

The data that support the findings of this study are available from the corresponding author upon reasonable request.

Keywords

digging, granular matter, insect cuticle, material wear, nanoindentation, oviposition

Received: July 26, 2024
Revised: September 9, 2024
Published online: September 23, 2024

[1] S. Amini, A. Miserez, *Acta Biomater.* **2013**, *9*, 7895.
[2] T. B. H. Schroeder, J. Houghtaling, B. D. Wilts, M. Mayer, *Adv. Mater.* **2018**, *30*, 1705322.
[3] M. Tadayon, O. Younes-Metzler, Y. Shelef, P. Zaslansky, A. Rechels, A. Berner, E. Zolotoyabko, F. G. Barth, P. Fratzl, B. Bar-On, Y. Politi, *Adv. Funct. Mater.* **2020**, *30*, 2000400.
[4] L. Kundanati, R. Guarino, N. M. Pugno, *Insects.* **2019**, *10*, 438.
[5] E. L. P. Dumont, C. Do, H. Hess, *Nat. Nanotech.* **2015**, *10*, 166.
[6] L. F. Martin, L. Krause, A. Ulbricht, D. E. Winkler, D. Codron, T. M. Kaiser, J. Müller, J. Hummel, M. Clauss, J. M. Hatt, E. Schulz-Kornas, *Palaeoecology.* **2020**, *556*, 109886.
[7] J. F. V. Vincent, U. G. K. Wegst, *Arthropod. Struct. Dev.* **2004**, *33*, 187.
[8] K. Stamm, B. D. Saltin, J. H. Dirks, *Appl. Phys. A: Mater. Sci. Process.* **2021**, *127*, 329.
[9] B. W. Cribb, A. Stewart, H. Huang, R. Truss, B. Noller, R. Rasch, M. P. Zalucki, *Naturwissenschaften.* **2008**, *95*, 433.
[10] Y. Zhang, C. Zhou, L. Ren, *J. Bionic Eng.* **2008**, *5*, 164.
[11] L. Cosme Jr, M. M. Haro, N. M. P. Guedes, T. M. C. Della Lucia, R. N. C. Guedes, *Pest Manage. Sci.* **2018**, *74*, 914.
[12] Y. Politi, M. Priewasser, E. Pippel, P. Zaslansky, J. Hartmann, S. Siegel, C. Li, F. G. Barth, P. Fratzl, *Adv. Funct. Mater.* **2012**, *22*, 2519.
[13] F. Püffel, O. K. Walthaus, V. Kang, D. Labonte, *Biol. Sci.* **2023**, *378*, 20220547.
[14] R. M. S. Schofield, K. D. Emmett, J. C. Niedbala, M. H. Nesson, *Behav. Ecol. Sociobiol.* **2011**, *65*, 969.

[15] V. Birkenfeld, S. N. Gorb, W. Krings, *Interface Focus.* **2024**, *14*, 20230048.
[16] C. L. Klunk, M. Heethoff, J. U. Hammel, S. N. Gorb, W. Krings, *Interface Focus.* **2024**, *14*, 20230056.
[17] U. G. K. Wegst, P. Cloetens, O. Betz, *Interface Focus.* **2024**.
[18] J. F. V. Vincent, *J. Entomol., Ser. A, Gen. Entomol.* **1976**, *50*, 175.
[19] R. Das, S. Gershon, B. Bar-On, M. Tadayon, A. Ayali, B. E. Pinchasik, *J. R. Soc., Interface.* **2022**, *19*, 20210955.
[20] R. Das, A. Ayali, M. Guershon, A. Ibraheem, E. Perlson, B. E. Pinchasik, *iScience.* **2022**, *25*, 105295.
[21] S. Gershon, B. Bar-On, S. Sonnenreich, A. Ayali, B. E. Pinchasik, *BMC Biol.* **2024**, *22*, 129.
[22] C. Klechevski, L. Kats, A. Ayali, *Sci. Nat.* **2024**, *111*, 43.
[23] M. S. Lehnert, K. E. Reiter, G. A. Smith, G. Kritsky, *Sci. Rep.* **2019**, *9*, 19731.
[24] J. Blackwell, M. A. Weih, *J. Mol. Biol.* **1980**, *137*, 49.
[25] N. Gundiah, S. Jaddivada, *Curr. Opin. Insect Sci.* **2020**, *42*, 84.
[26] D. L. J. Quicke, M. G. Fitton, *Proc.: Biol. Sci.* **1995**, *261*, 99.
[27] U. Cerkvenik, B. van de Straat, S. W. S. Gussekloo, J. L. van Leeuwen, *Proc. Natl. Acad. Sci. USA.* **2017**, *114*, E7822.
[28] G. Ramesh, G. Gokilakrishnan, V. C. Uvaraja, S. Santhosh Kumar, *Biomass Conv. Bioref.* **2024**, https://doi.org/10.1007/s13399-024-05345-3.
[29] W. Zhai, L. Bai, R. Zhou, X. Fan, G. Kang, Y. Liu, K. Zhou, *Adv. Sci.* **2021**, *8*, 2003739.
[30] Y. Politi, B. Bar-On, H. O. Fabritius, *Architectured Materials in Nature and Engineering: Archimats*, (Eds.: Y. Estrin, Y. Bréchet, J. Dunlop, P. Fratzl), Springer International Publishing, Cham, Switzerland **2019**, pp. 287–327.
[31] C. Li, S. N. Gorb, H. Rajabi, *Acta Biomater.* **2020**, *103*, 189.
[32] J. Michels, S. N. Gorb, *J. Microsc.* **2012**, *245*, 1.
[33] A. C. Croce, *Photochem.* **2021**, *1*, 67.
[34] F. Alhousari, M. Greger, *Plants.* **2018**, *7*, 33.
[35] F. P. Massey, S. E. Hartley, *J. Anim. Ecol.* **2009**, *78*, 281.
[36] F. P. Massey, A. R. Ennos, S. E. Hartley, *J. Anim. Ecol.* **2006**, *75*, 595.
[37] P. A. Calatayud, E. Njuguna, J. Gerald, *Entomol., Ornithol. Herpetol.: Curr. Res.* **2016**, *5*, e125.
[38] C. Li, S. N. Gorb, H. Rajabi, *Beilstein J. Nanotechnol.* **2022**, *13*, 404.
[39] D. Klocke, H. Schmitz, *Acta Biomater.* **2011**, *7*, 2935.
[40] S. Bentov, P. Zaslansky, A. Al-Sawalmih, A. Masic, P. Fratzl, A. Sagi, A. Berman, B. Aichmayer, *Nat. Commun.* **2012**, *3*, 839.
[41] S. O. Andersen, *Insect Biochem. Mol. Biol.* **2010**, *40*, 166.
[42] R. W. van Nieuwenhoven, M. Drack, I. C. Gebeshuber, *Adv. Funct. Mater.* **2024**, *34*, 2307127.
[43] A. E. Vellwock, A. Narkevicius, C. Fischer, O. Spaecker, European Synchrotron Radiation Facility **2026**, https://doi.org/10.15151/ESRF-ES-1030394505.
[44] F. Pedregosa, G. Varoquaux, A. Gramfort, V. Michel, B. Thirion, O. Grisel, M. Blondel, P. Prettenhofer, R. Weiss, V. Dubourg, J. Vanderplas, A. Passos, D. Cournapeau, M. Brucher, M. Perrot, É. Duchesnay, *JMLR.* **2011**, *12*, 2825.